The effects of the “Mega-drought” in small periglacial mountain streamlets (Dry-Central Andes of Argentina)

Martín Mendoza[1], Carla Tapia Baldis[1], Dario Trombotto Liaudat[1] & Noelia Sileo[2]

[1]*IANIGLA: Instituto Argentino de Nivología, Glaciología y Ciencias Ambientales, CCT Conicet, Mendoza, Argentina*

[2]*CNEA: Comisión Nacional de Energía Atómica PNGRR, Regional Cuyo, Mendoza, Argentina*

ABSTRACT

In the Dry-Central Andes of Argentina (31° to 35°S), hydrological systems are cryospheric, influenced by variable snowfall, and shaped by solid-state water reservoirs. Permafrost is expected between 3400 and 4200 m asl under favorable topographic conditions. Since 2010, a strong hydrological drought, caused by reduced precipitations and rising air temperatures, impacted small mountain stream discharges. The Chasquillar basin (31°45'S and 70°15'W), displays periglacial landforms in its upper part at 3800 m asl, such as active and transitional rock glaciers. Glacial moraines cover the middle and the lower part, where the Chasquillar streamlet flows. This small mountain streamlet has a perennial flow, fed by a spring with a surrounding wetland ecosystem. Since 2018, hydrological parameters were monitored in the field, with the aim of elucidate the interplay between the meteorological variables and the flow dynamics under the drought conditions. Using a site-specific calibration equation, discharge was calculated from water level, measured with a data logger placed in a metallic cutthroat-flume gauge station. The device recorded data every 4 hours between April 2018 and April 2023. Soil moisture and temperature were monitored upstream from the spring sampling point between April 2019 to April 2023, at depths from 0 to 80 cm. Results show a peak discharge of 20-30 l/s but, between April 2019 to October 2022, it remained at 4–5 l/s (base flow), with seemingly small contributions from snow melting, due to the “Mega-drought” condition.

1 INTRODUCTION

The Central Andes of Argentina and Chile (31–35°S) comprise the largest periglacial continental belt in the southern hemisphere (Gruber 2012). The cycles of freezing and thawing that occur extensively in cold regions, as well as the distribution of permafrost, influence runoff distribution, groundwater flows, and the physical-chemical processes. In this region, water sources primarily result from the summer (dry season) melting of snow and glaciers (Corte 1983; Masiokas et al. 2010). These sources include contributions from seasonally frozen soils and permafrost, each playing distinctive hydrological roles (Schaffer et al. 2019; Hayashi 2020). A central element of the periglacial hydrological system is the active layer. Some authors refer to this unit as a temporary or seasonal aquifer (Halla et al. 2021; Liaudat et al. 2020), as it stores water during the cold months in the form of seasonal ground ice, releasing it during the summer as the thawing front penetrates the soil.

Climate trends for the Central Andes forecast drastic decreases in surface water supply, resulting from a combination of various factors. Since 2010, the region has been experiencing what is referred to as a "mega-drought (hydrological)" (Garreaud et al. 2020; Rivera et al. 2021). One of the primary contributors to this phenomenon is the reduction in the duration and extent of seasonal snow cover in mountainous regions, as the global average temperature continues to rise (Zazulie et al. 2018). According to the latest reports, the air temperature in mountainous regions at a global scale shows an increase ranging from 0.1 to 0.3 °C per decade throughout the 21st century (Biskaborn et al. 2019; Hock et al. 2019). For the Central Andes, the trend between 1991 and 2021 was +0.2 °C per decade and it is projected to continue rising to +2 °C between 2024 and 2048 under an SSP-1 scenario (Caragunis et al. 2020). There is evidence that in some regions of the world, the threshold for peak water has been exceeded, especially in areas where ice bodies are small, such as the Central and Southern Andes, western Canada, and the Alps. Consequently, it is expected that the solid water reserves in mountainous regions (snow, glaciers, and frozen soils) will continue to experience high environmental stress. As glaciers retreat and eventually disappear, the role of frozen soils and permafrost in the hydrology of mountain systems will become increasingly significant for the water balance. The trend is toward a modification of the hydrological system, shifting from snow/glacier-dominated dynamics to periglacial ones (Haeberli et al. 2019; Arenson et al. 2022). The periglacial environment response shows a dynamic behaviour, responding differently to climate variability. The hydrological significance of rock glaciers in the Central Andes has been explored by numerous authors, often in relation to discharge prediction (Schrott 1991; Trombotto et al. 1997), and this subject has been a topic of discussion at both regional and global scales (Arenson and Jakob 2010; Duguay et al. 2015; Trombotto-Liaudat and Bottegal 2020). Recent studies have contributed to quantifying the water storage capacity of rock glaciers, clarifying their role in the hydrological cycle, and interpreting various flows within the periglacial system (Arenson et al. 2022; Halla et al. 2021; Hilbich et al. 2022; Hoelzle et al. 2022; Liaudat et al. 2020; Sileo et al. 2020).

1.1 Objectives

The aim of this study is to comprehensively examine the hydrology of a periglacial mountain basin situated in the Central Dry Andes of Argentina. Our objective is to analyze the behavior of the hydrological system in years of drought and periods of increased precipitation. This will be achieved by distinguishing between yearly segments of accumulation

https://doi.org/10.52381/ICOP2024.133.1

and recession in the discharge hydrological data. For each period, regression analyses from 'wet' and 'dry' years could be explained in terms of the meteorological variables. Specifically, we seek to gain a deeper understanding of the crucial roles played by periglacial Andean processes, including snowmelt, soil freezing and thawing, and groundwater discharge across the aforementioned basin.

1.2 Study Area

The study area is situated on the western slope of the Santa Cruz Mountain range (Central Andes of Argentina), spanning coordinates 31°45'S and 70°12'W to 31°48'S and 70°15'W and an elevation range spanning from 3400 m asl to 4800 m asl. The “Chasquillar” valley conforms a north-northeast to south-southwest elongated valley, which acts as a minor tributary of the Santa Cruz River, a permanent stream with a mean module of 306 l/s (Figure 1).

The geomorphology of the study area exhibits three distinct altitudinal segments. Periglacial processes, resulting in widespread landforms such as rock glaciers, protalus ramparts, soli-gelifluction slopes, and cryoplanation terraces, dominate the upper section (Figure 2). These features collectively constitute 25% of the total basin surface. The middle section displays landforms of ancient glacial origin. The valley bottom contains till deposits and till exhibiting cryogenic characteristics, accounting for 12% of the total area. Although fluvioglacial units cover a mere 1% of the landscape, it is inferred that they play a significant role in the basin’s hydrogeology. Detrital slopes encompass 12% of the total area, while additional units of gravitational and alluvial origin make up 7%.

The lower basin section accommodates a main permanent streamlet, primarily fed by a spring surrounded by meadows colloquially referred to as the "Chasquillar" stream. In this portion, the prevailing features are mainly detrital slopes and ancient glacial deposits. Noteworthy within the basin's topography is a slope discontinuity between the second and third segments, marked by a moraine front approximately 100 m in thickness. This moraine front suggests distinct ice advances during the Quaternary period.

According to the Köppen classification, the climate is polar tundra of high-altitude (ETH), with minimum to null excess water, scarce summer precipitation, and permafrost presence. Annually, the thawing season with monthly mean air temperatures > 0 °C extends from November to April, while the freezing season starts in May and lasts to December. The precipitation patterns show a well-defined seasonal regime, with maximum precipitation during the cold season and scarce precipitation during the warm season. Precipitation is nival, with annual means ranging from 300 to 400 mm (Arenson et al. 2010), being strongly controlled by the phase of El Niño Southern Oscillation (ENSO) (Montecinos and Aceituno, 2003), with annual maximums of 1100–1200 mm during its occurrence. The mean annual air temperature (MAAT) at approximately 3600 m asl is 0.18 °C; during the thawing season MAAT ascends up to 7.2 °C, descending down to -5.43 °C during the cold season. Mean air temperature in the coldest month (July) was -11.55 °C at 3600 m asl, with a historical minimum close to -30 °C during July of 2000.

Various lithological units are exposed in the area, predominantly pyroclastic rocks of rhyolitic composition (Rancho de Lata formation), volcanic andesites (Choiyoi group), and porphyritic rocks of andesitic/dacitic composition (Farellones formation intrusive). Secondary hydrothermal alteration minerals have affected a portion of the area.

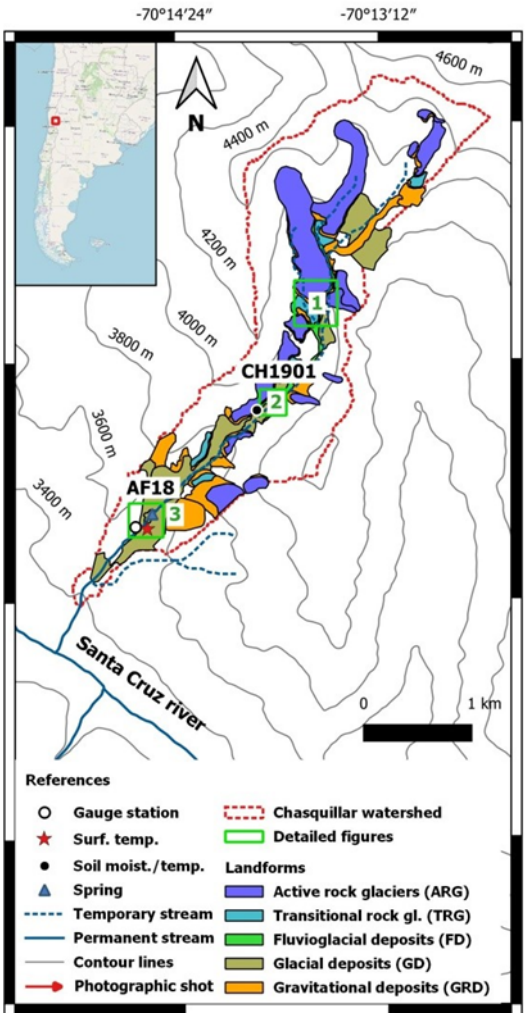

Figure 1. Geomorphology of the Chasquillar basin, displaying main landforms and drainage network. Sampling and instrumentation points are shown.

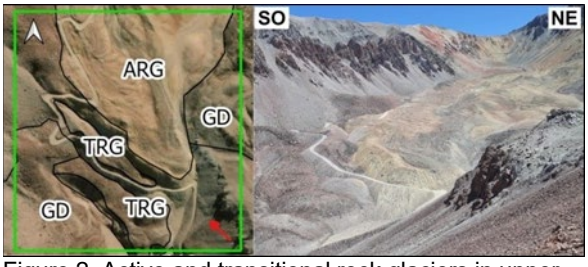

Figure 2. Active and transitional rock glaciers in upper section of the basin (see reference for detailed Figure 1).

2 METHODS

2.1 Field Instrumentation

2.1.1 Flume design

We installed a "cutthroat flume" structure at the chosen site (AF18 3480 m asl) with the following design specifications: it is a cutthroat flume measuring 10 cm in width (*W*) and 90 cm in length (*L*), constructed from 2 mm thick iron plate with reinforcements. Here, *W* represents the throat width, and *L* represents the total length of the flume (Figure 3).

Figure 3. "Cutthroat flume" in the Chasquillar streamlet, at the lower section of the homonymous basin (see reference for detailed figure 3).

The theoretical calculation of discharge in a cutthroat flume, assuming free-flow conditions, can be determined using the following formula:

$$Q = C \times {H_a}^n \quad [1]$$

In this equation, *Q* represents the discharge in cubic meters per second (m³/s), *C* is the coefficient of free flow, H_a (m) is the water level measured upstream at a distance from the throat equal to 2/9L (m), and *n* is the exponent of the equation.

For the specific geometric design mentioned, the equation can be expressed as:

$$Q = 0.35 \times {H_a}^{1.84} \quad [2]$$

After the installation of the flume, a calibration test was conducted using the salt dilution gauging method. This test yielded four discharge measurements corresponding to different values of H_a (water level). The calibration range spanned from 4.84 liters per second (l/s) to 7.10 l/s.

Based on the test results, an empirical adjustment of the coefficients *C* and *n* was performed to align the flume equation with the observed relationship between Q (discharge) and H_a. As a result, the calibrated flume equation is as follows:

$$Q = 0.13 \times {H_a}^{1.5} \quad [3]$$

2.1.2 Water discharge

In this study, we employed a HOBO U20L-04 data logger, placed inside a watertight chamber attached to the flume channel, as illustrated in Figure 3. This chamber is hydraulically connected to the flume through a slot located at the $H_a$reading site. The data logger is designed to operate within a pressure range of 0 to 4 m of water (at sea level) and can function in temperatures ranging from -20 °C to 50 °C. It provides precise measurements of absolute pressure with an accuracy of ± 0.4 cm H_20 and a resolution of 0.14 cm H_20. Additionally, it measures water temperature with an accuracy of ± 0.44 °C and a resolution of 0.10 °C. Data from this equipment were collected continuously from April 2018 to April 2023, with readings taken at intervals of 4 hours. At the measurement point H_a, we determined the hydrostatic pressure by calculating the difference between the absolute pressure recorded by the HOBO U20L-04 sensor and the atmospheric pressure. These measurements were expressed in meters of water, converting them into the corresponding discharge rates using the flume calibrated curve (equation 3).

We created a hydrograph illustrating the discharge rates observed in the Chasquillar stream (site AF18) from 2018 to 2023, accompanied by water temperature readings. To filter the discharge curve, we applied the following criteria during specific periods:

a) When the water column was completely frozen, as indicated by the bottom-of-the-flume water temperature readings, we considered a maximum depression of the freezing point equal to -0.09 °C.
b) During periods when the top of the water column was frozen, we identified intervals on which the water temperature remained steady and variability tended to be minimal, a phenomenon referred to as the "zero curtain".

After filtering, we classified the discharge rates into their respective hydrological years. Each hydrological year was further divided into two intervals:

1) The accumulation interval, starting from the beginning of the series and extending to the point of maximum discharge.
2) The recession interval, starting from the point of maximum discharge and concluding at the start of an extended freezing period in the stream.

2.1.3 *Recession curves*

The recession intervals of the hydrograph were analyzed in terms of aquifer discharge, which can be represented by an exponential equation with a negative exponent in the form of:

$$Q_t = Q_0 e^{-\propto t} \quad [4]$$

Here, Q_0 represents the initial discharge, Q_t the discharge at time t, $\propto$ the coefficient of the aquifer and e, the base of the natural logarithm.

In complex aquifers, the recession can be interpreted by a function that is the sum of several exponential segments, where the intervals represent different stages in the drainage process.

2.1.4 *Soil temperature and moisture content*

At site CH19, we deployed four Truebner SMT100 sensors to measure soil temperature and soil volumetric water content (VWC) at different depths (0.05 m, 0.2 m, 0.5 m, and 0.8 m; Figure 4). These sensors were connected to a data logger that collected data every 4 hours from April 2019 to April 2023. The sensors have an accuracy of ± 3% for VWC and ± 0.2 °C for temperature in mineral soils, with a resolution of 0.1% for VWC and 0.01 °C for temperature. After deploying the sensors at the specified depths, we filled the pit with sediments extracted during excavation.

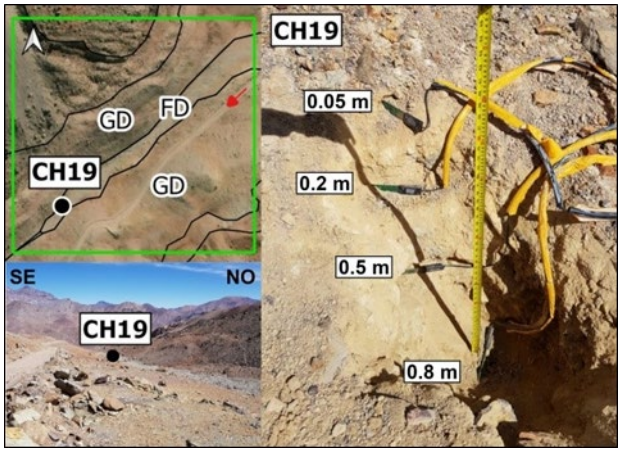

Figure 4. Site CH19, with SMT-100 sensors to measure soil temperature and soil volumetric water content at different depths (see reference for detailed Figure 2).

2.1.5 *Meteorological data sources*

For various meteorological variables, we relied on gridded data series obtained from global reanalysis models to compensate for the lack of instrumental data in the study area. Although there are meteorological stations near the study area, these stations only have historical records, and the most recent data are either sporadic or unavailable. The selected reanalysis models covered the following variables:

- Air temperature was represented using the ERA5 model.
- Rainfall data were derived from the ERA5 model.
- Snow cover thickness was obtained from the ERA5-AG model.
- Atmospheric pressure was determined using the NCEP NNRP model, specifically the flow subset R1 (2D) with a forecast every 6 hours. The grid had a resolution of 1.875° x 1.904° and covered surface-level data.

All the mentioned gridded data series were validated through correlation analysis with historical records from the nearest meteorological station, Pachón (31°45'34.60"S and 70°24'45.30"W)

2.1.6 *Correlation and multivariable regression analysis*

Using the "sample cross correlation function (CCF)" tool within R, we analyzed meteorological variables to define the degree of correlation with the discharge curve in the accumulation intervals, considering their possible delays (lag).

3 RESULTS

3.1 "Mega drought" meteorological settings

Compared to a reference period (2010–2023), the years 2018 to 2023 were warmer and dryer. The warmest years were 2019 and 2020 (mild El Niño anomaly), with MAATs of 0.89 and 0.79 °C, representing anomalies of +2.0 °C and +1. 8°C, respectively (at 3704 m asl). Moreover, no negative air temperature anomaly was recorded since the coldest year 2010 (-0.3 °C anomaly); all the remaining years showed positive temperature anomalies (Figure 5 and Table 1). The same trend was also observed at the soils, that displayed exceptionally high temperatures with MAGTs above 4.0 °C (at 20 cm depths) during the whole observation period.

Regarding the precipitation, the year 2019 was the driest of the whole period, with a precipitation anomaly of -180 mm/yr, compared to a mean value of 280 mm/yr (1981–2021). Since 2010, precipitation records have always shown a deficit, especially notorious in the winter-accumulated values (Table 1). In the soil moisture profile, seasonally, periods with a negative gradient (moisture decreases with depth) occur during snowmelt and soil thawing, while positive gradient periods occur during late summer and the onset of soil freezing.

Table 1. Summary of meteorological variables during 2018–2023 at 3704 m asl.

	18/19	19/20	20/21	21/22	22/23
MAAT (°C)	-0.20	0.89	0.79	-0.02	-0.83
MAAT Anomaly (°C)	+0.9	+2.0	+1.8	+1.2	+0.8
MAGT (°C)	-	5.13	4.51	4.62	4.01
Mean T° Warm season (°C)	10.24	9.76	8.83	10.56	8.70
Mean T° Cold season (°C)	-10.17	-8.61	-8.71	-10.57	-9.49
Annual Precip. (mm/yr)	453.73	311.93	439.86	333.57	401.65
Precip. Anomaly (mm/yr)	-105	-180	-160	-170	-100
Summer Precip. (mm/yr)	113.20	89.36	168.94	165.24	50.29
Winter Precip. (mm/yr)	329.72	257.79	159.57	155.87	334.54
Snow coberture (%)	52.43	38.29	36.81	33.20	49.52
Accumulated snow (mm)	2495	1345	1804	1143	2326

3.2 Discharge analysis

Peak streamflow occurs in mid-December to late-April and is due to snowmelt rather than summer rainfall. The dominance of seasonal snowmelt creates a hydrograph with a steep rising limb and gradual recessional limb. In terms of water discharge from the Chasquillar streamlet, two distinctive periods were observed: “wet” years (2018–2019 and 2022–2023), versus “dry” years (2019–2022).

In wet years, the average flow ranges from 7.8 to 9.2 l/s, while maximum flows range from 30.1 to 23.5 l/s. In dry years, the average flow ranges from 1.7 to 2.9 l/s, while maximum flows range from 5 to 5.3 l/s. In the first case, the peak discharge occurs in December (beginning of the austral summer), whereas in dry years, the streamflow curve is very stable, and the maximum flow occurs between March and April (austral autumn; Figure 5 and Table 2).

Regarding water temperature, the freezing period occurs at the beginning of each hydrological year, typically lasting between 80 and 89 days. In the year 2021–2022, it had a shorter duration. Moreover, in wet years, the low flow period (< 5 l/s) occurs at the end of winter (freezing period) and before snowmelt leads to an increase in flow. It represents between 25% (2018–2019) and 38% (2022–2023) of the streamflow curve. In dry years, the entire curve remains below 5 l/s (Table 2).

Table 2. Summary of meteorological hydrological variables during 2018–2023 at site AF18.

Hydrological Year	18/19	19/20	20/21	21/22	22/23
Duration (days)	353	372	382	383	-
Freezing period (days)	89	80	89	106	81
Accumulation period (days)	114	240	177	211	105
Recession period(days)	145	36	96	65	-
Min. discharge (l/s)	0.94	0.5	0.47	0.13	4.96
Max. discharge (l/s)	23.54	5.33	5.13	4.96	30.15
Avg. discharge	9.18	2.9	2.93	1.7	7.83
High flow duration (days)	192	-	-	-	147
Low flow duration (days)	67	276	273	276	91

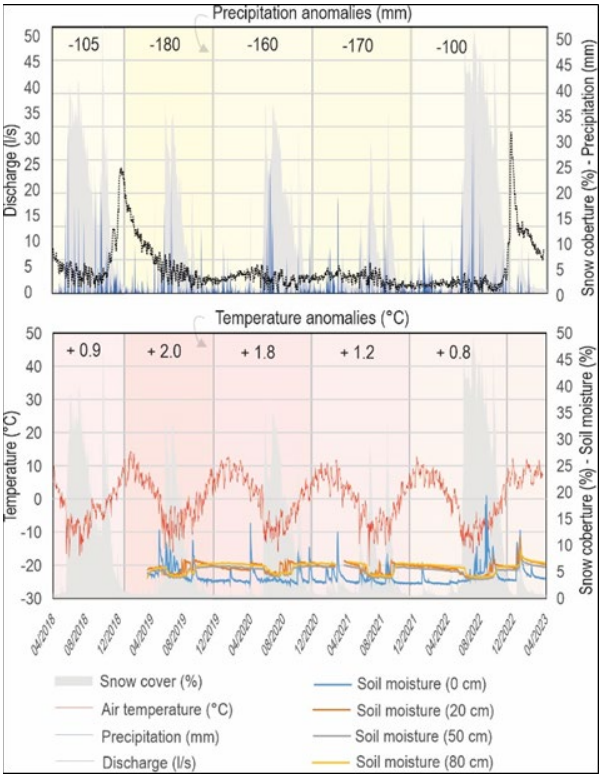

Figure 5. Daily values of water discharge (l/s), precipitation (mm/day) and snow cover (%) at AF18 site (upper figure). Down: daily air temperature records (°C) and soil moisture content (%) at site CH19.

3.3 Recession curves and regression analysis

In wet years, the accumulation (related to snowmelt) and recession (related to groundwater discharge) periods of the flow curve are well defined. For the year 2018–2019, the

accumulation period lasted 114 days. The recession of this hydrological year can be divided into two segments: the first segment comprises the first 22 days of recession, with an alpha value of -0.019, and the second recession segment spans 99 days, with an alpha value of -0.009 (Figure 6). For the year 2022–2023, the accumulation period lasted 105 days. The recession of this hydrological year, divided into two segments, results in a first segment comprising the first 24 days of recession, with an alpha value of -0.036, and the second recession segment spans 109 days, with an alpha value of -0.008 (Figure 6). It is important to emphasize the similarity in the alpha value for the second segment of recession in the two analyzed wet years. This could be considered an indicator of the properties of the basin's aquifers.

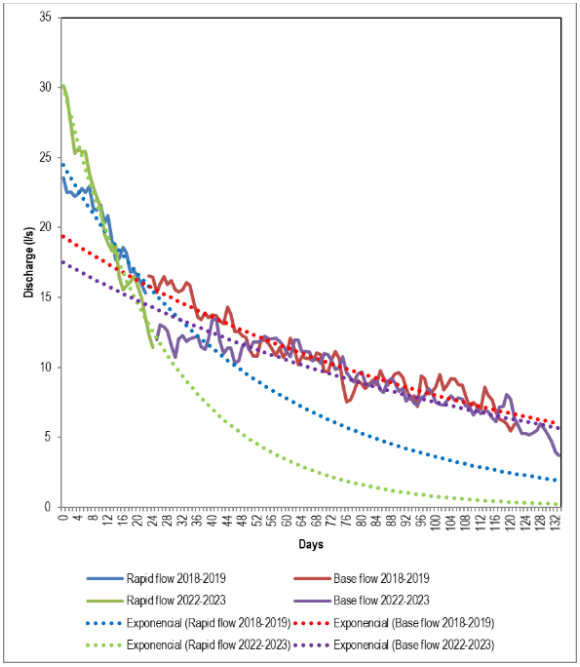

Figure 6. Recession curves during the “wet” years and best fitting model.

In wet years, the accumulation segment of the discharge curve can be explained in terms of the following meteorological variables: snow depth, precipitation, and air temperature, with R-squared values ranging from 0.86 (2018–2019; Table 3) to 0.63 (2022–2023; Table 4). In the year 2022–2023, the soil temperature at a depth of 80 cm is also a significant predictor in the regression model. Soil moisture at a depth of 20 cm shows a negative relationship with streamflow, primarily evident in dry years (R-squared equal to 0.4 in the year 2019–2020, with a lag of 15 days). In wet years, there is no significant relationship between soil moisture and the streamflow curve.
On the other hand, in dry years, the correlation between discharge and the mentioned meteorological variables is negligible (R-squared between 0.16 and 0.18), except for the year 2020–2021, in which snowfall was slightly more intense, and the correlation with meteorological variables reaches 0.58.

Table 3. Accumulation model for 2018–2019 “wet” period.

	Estimate	Std. Error	T value	Pr(>|t|)
Intercept	8.86	0.62	14.39	<2e-16
Snow depth	-0.01	0.001	-4.77	5.7e-06
Precipitation	1.78	0.21	8.38	2.1e-13
Air temperature	0.66	0.11	5.75	8.3e-08
	Residuals	Multiple R-squared		0.86
Min	-5.95	p-value		< 2,2e-16
1Q	-1.58			
Median	-0.22			
3Q	0.99			
Max	8.57			

Table 4. Accumulation model for 2022–2023 “wet” period.

	Estimate	Std. Error	T value	Pr(>|t|)
Intercept	-4.27	0.98	-4.37	3.5e-0.5
Snow depth	0.01	0.001	8.90	2.4e-14
Precipitation	0.54	0.1	4.00	1.2e-04
Air temperature	0.34	0.13	2.41	1.8e-02
Soil temp. 0.8 m	1.94	0.25	7.88	4.01e-12
	Residuals	Multiple R-squared		0.78
Min	-9.11	p-value		<2.2e-16
1Q	-1.45			
Median	0.15			
3Q	1.07			
Max	12.64			

4 DISCUSSION

During 2019–2022, the precipitations below the average were simultaneous with positive anomalies of winter temperatures, interrupting the seasonal freezing in the upper part of the basin (above 3800 m asl). Then, the scarce accumulated snow melted in the middle of winter and meltwater flowed into the uppermost part of the active layer, introducing heat into the ground, and so decreasing the freezing depth. By the beginning of the snow-melting period in November, the accumulated snow is very thin, melting quickly and percolating, but soil water does not reach the saturation point. If the snow coverture threshold is below a 30%, in terms of basin surface; and soil moisture below 10%, not enough snowmelt water is available to produce a discharge and no peak-flow is observed.

The recorded water discharges in the Chasquillar streamlet during “dry” years, were similar to the ones found at the tongue of the “Dos Lenguas” rock glacier, in the Dry Andes (Schrott 1991), of 5–6 l/s. When comparing with the Vallecitos basin, in the Central Andes of Mendoza, the average discharge flow (1991–1993) was much higher: 500 l/s during wet years (Trombotto et al. 1997; Sileo 2019). Other studies obtain discharge values from rock glacier-fed basins varies between ~5 and ~250 l/s (Harrington et al. 2018; Krainer and Mostler 2002). As in many other studies,

the seasonal variations in discharge occur with the lowest flows observed in winter, consisting mostly, if not completely, of base flow (Burger et al. 1999; Krainer et al. 2007).

Under stable permafrost conditions, the contribution from interstitial thaw to surface runoff is extremely small/negligible, for example Krainer et al. (2015), found an average annual rate of ground ice melt from thawing permafrost of 10 cm/year, which represented only 2.3% of the average discharge from the rock glacier catchment area. However, the contribution to the runoff from permafrost thaw can change in response to climate shifts. Local permafrost maps could enhance the interpretation of these findings, again, in terms of any likely spatial gradient therein.

5 CONCLUSIONS

This study lacks measurements for the soil water content at depth > 1 m. Because of the observed relationship between streamflow and meteorological variables in wet years, we can interpret the main sources of water in the Chasquillar basin: snowmelt and late-season precipitation are two significant components that together explain part of the observed variability. Furthermore, the relationship between streamflow with air temperature, and particularly with soil temperature, can be interpreted as indicators of the role played by soil thawing in the accumulation phase of the streamflow curve. The segmentation observed in recession curves can be interpreted in terms of a fast-flow component, which manifests in the first 25 days after the peak flow, and a slow-flow component corresponding to groundwater discharge.

The lack of correlation between soil moisture and streamflow suggests that the sources feeding the Chasquillar stream are primarily controlled by underground flows, which have an indirect relationship with surface infiltration in the upper and middle parts of the basin. However, in years with diminished total snow accumulation and melt, it is expected that there will be a
decrease in groundwater recharge, that in turn will decrease the peaks of groundwater discharge to the streams.

6 ACKNOWLEDGEMENTS

This study was funded by the project PIP 1222015-0100913, granted by the Consejo Nacional de Investigaciones Científicas y Técnicas (CONICET), and the project PICT-2019-03799 granted by the Agencia Nacional de Promocion de la Investigación, el Desarrollo Tecnológico y la Innovacion. The authors express their gratitude to Silvio Pastore, Jorge García, and Dino Taillant for their valuable help during field tasks.

7 REFERENCES

Arenson, L.U. and Jakob, M. 2010. 'The significance of rock glaciers in the dry Andes - A discussion of Azócar and Brenning (2010) and Brenning and Azócar (2010)', *Permafrost Periglacial Process* 21, pp. 282–285. Available at: https://doi.org/10.1002/ppp.693.

Arenson, L.U., Pastore, S., Liaudat, D.T., Bolling, S., Quiroz, M.A., and Ochoa, X.L. 2010. 'Characteristics of two Rock Glaciers in the Dry Argentinean Andes Based on Initial Surface Investigations', in *Proceedings GEO2010*, 63rd Canadian Geotechnical Conference & 6th Canadian Permafrost Conference. Calgary, Alberta, Canada: pp. 1501–1508.

Arenson, L.U., Harrington, J.S., Koenig, C.E.M., and Wainstein, P.A. 2022. 'Mountain Permafrost Hydrology—A Practical Review Following Studies from the Andes', *Geosciences* 12(2), 48. Available at: https://doi.org/10.3390/geosciences12020048.

Biskaborn, B.K., Smith, S.L., Noetzli, J., Matthes, H., Vieira, G., Streletskiy, D.A., et al. 2019. 'Permafrost is warming at a global scale', *Nature Communications*, 10(1), 264. Available at: https://doi.org/10.1038/s41467-018-08240-4.

Burger, K.C., Degenhardt, J.J., and Giardino, J.R. 1999. 'Engineering geomorphology of rock glaciers', *Geomorphology*, 31(1), pp. 93–132. Available at: https://doi.org/10.1016/S0169-555X(99)00074-4.

Caragunis, J., Rivera, J., and Penalba, O. 2020. 'Characterisation of hydrological droughts in central north Argentina and their atmospheric and oceanic drivers', *Climate Research*, 80(1), pp. 1–18. Available at: https://doi.org/10.3354/cr01593.

Corte, A. 1983. *Geocriología*. El frío en la Tierra., Ediciones Culturales de Mendoza (ed.), Mendoza, Argentina.

Duguay, M., Edmunds, A., Arenson, L., and Wainstein, P. 2015. 'Quantifying the significance of the hydrological contribution of a rock glacier – A review' in *GEOQuebec 2015,* 68th Canadian Geotechnical Conference & 7th Canadian Permafrost Conference. Québec City, Québec, Canada: 8 p.

Garreaud, R.D., Boisier, J.P., Rondanelli, R., Montercinos, A., Sepúlveda, H.H., and Veloso-Aguila, D. 2020. 'The Central Chile Mega Drought (2010–2018): A climate dynamics perspective', *International Journal of Climatology* 40, pp. 421–439.

Gruber, S. 2012. 'Derivation and analysis of a high-resolution estimate of global permafrost zonation', *The Cryosphere* 6, pp. 221–233. Available at: https://doi.org/10.5194/tc-6-221-2012.

Haeberli, W., Oerlemans, J., and Zemp, M. 2019. 'The Future of Alpine Glaciers and Beyond', *Oxford Research Encyclopedia of Climate Science*. Available at: https://doi.org/10.1093/acrefore/9780190228620.013.769.

Halla, C., Blöthe, J.H., Tapia Baldis, C., Trombotto Liaudat, D., Hilbich, C., Hauck, C., Schrott, L. 2021. 'Ice content and interannual water storage changes of an active rock glacier in the dry Andes of Argentina', *The Cryosphere* 15, pp. 1187–1213. Available at: https://doi.org/10.5194/tc-15-1187-2021.

Harrington, J.S., Mozil, A., Hayashi, M., and Bentley, L. R. 2018. 'Groundwater flow and storage processes in an inactive rock glacier', *Hydrological Processes*, *32*(20), pp. 3070–3088. Available at: https://doi.org/10.1002/hyp.13248.

Hayashi, M. 2020. 'Alpine Hydrogeology: The Critical Role of Groundwater in Sourcing the Headwaters of the World', *Groundwater* 58, pp. 498–510. Available at: https://doi.org/10.1111/gwat.12965.

Hilbich, C., Hauck, C., Mollaret, C., Wainstein, P., and Arenson, L.U. 2022. 'Towards accurate quantification of ice content in permafrost of the Central Andes – Part 1: Geophysics-based estimates from three different regions'. *The Cryosphere*, 16(5), pp. 1845–1872. Available at: https://doi.org/10.5194/tc-16-1845-2022.

Hock, R., Rasul, G., Adler, C., Cáceres, B., Gruber, S., Hirabayashi, M., et al. 2019. 'Chapter 2: High Mountain Areas' in H.-O. Pörtner, D.C. Roberts, V. Masson-Delmotte, P. Zhai, M. Tignor, E. Poloczanska, K. Mintenbeck, A. Alegría, M. Nicolai, A. Okem, J. Petzold, B. Rama, N.M. Weyer (eds.) *IPCC Special Report on the Ocean and Cryosphere in a Changing Climate*. Cambridge, UK: Cambridge University Press, pp. 181–202. Available at: https://doi.org/10.1017/9781009157964.004.

Hoelzle, M., Hauck, C., Mathys, T., Noetzli, J., Pellet, C., and Scherler, M. 2022. 'Long-term energy balance measurements at three different mountain permafrost sites in the Swiss Alps', *Earth System Science Data* 14(4), pp. 1531–1547. Available at: https://doi.org/10.5194/essd-14-1531-2022.

Krainer, K. and Mostler, W. 2002. 'Hydrology of Active Rock Glaciers: Examples from the Austrian Alps', *Arctic, Antarctic, and Alpine Research*, *34*(2), pp. 142–149. Available at: https://doi.org/10.1080/15230430.2002.12003478.

Krainer, K., Bressan, D., Dietre, B. et al. 2015. 'A 10,300-year-old permafrost core from the active rock glacier Lazaun, southern Ötztal Alps (South Tyrol, northern Italy)', *Quaternary Research* 83, pp. 324–335.

Krainer, K., Mostler, W., and Spötl, C. 2007. 'Discharge from active rock glaciers, Austrian Alps: A stable isotope approach', *Austrian Journal of Earth Sciences* 100, pp. 102–112.

Liaudat, D.T., Sileo, N., and Dapeña, C. 2020. 'Periglacial water paths within a rock glacier-dominated catchment in the Stepanek area, Central Andes, Mendoza, Argentina'. *Permafrost and Periglacial Process* 31, pp. 311–323. Available at: https://doi.org/10.1002/ppp.2044.

Masiokas, M.H., Villalba, R., Luckman, B.H., and Mauget, S. 2010. 'Intra- to Multidecadal Variations of Snowpack and Streamflow Records in the Andes of Chile and Argentina between 30° and 37°S', *Journal of Hydrometeorology* 11, pp. 822–831. Available at: https://doi.org/10.1175/2010JHM1191.1.

Montecinos, A. and Aceituno, P. 2003. 'Seasonality of the ENSO-Related Rainfall Variability in Central Chile and Associated Circulation Anomalies', *Journal of Climate*,16(2), pp. 281–296. Available at: https://doi.org/10.1175/1520-0442(2003)016<0281:SOTERR>2.0.CO;2.

Rivera, J.A., Otta, S., Lauro, C., and Zazulie, N. 2021. 'A Decade of Hydrological Drought in Central-Western Argentina', *Frontiers in Water* 3, 640544. Available at: https://doi.org/10.3389/frwa.2021.640544.

Schaffer, N., MacDonell, S., Réveillet, M., Yáñez, E., and Valois, R. 2019. 'Rock glaciers as a water resource in a changing climate in the semiarid Chilean Andes', *Regional Environmental Change* 19, pp. 1263–1279. Available at: https://doi.org/10.1007/s10113-018-01459-3.

Schrott, L., 1991. 'Global solar radiation, soil temperature and permafrost in the Central Andes, Argentina: A progress report'. *Permafrost and Periglacial Processes* 2, pp. 59–66. Available at: https://doi.org/10.1002/ppp.3430020110.

Sileo, N.R. 2019. *Estudio del comportamiento hidrogeoquímico de las aguas subterráneas y superficiales relacionadas con glaciares, glaciares cubiertos y glaciares de escombros, en la cuenca del río Vallecitos, Cordillera Frontal, Mendoza*. Universidad Nacional de Buenos Aires (UBA).

Sileo N.R., Dapeña C., and Trombotto Liaudat D. 2020. 'Isotopic composition and hydrogeochemistry of a periglacial Andean catchment and its relevance in the knowledge of water resources in mountainous areas', Isotopes in Environmental and Health Studies. Available at: https://doi.org/10.1080/10256016.2020.1814278.

Trombotto-Liaudat, D. & Bottegal, E. 2020. 'Recent evolution of the active layer in the Morenas Coloradas rock glacier, Central Andes, Mendoza, Argentina and its relation with kinematics', *Cuad. Investig. Geográfica* 46, pp. 159–185.

Trombotto, D., Buk, E., and Hernández, J. 1997. 'Monitoring of Mountain Permafrost in the Central Andes, Cordon del Plata, Mendoza, Argentina', *Permafrost and Periglacial Processes* 8(1), pp. 123–129.

Zazulie, N., Rusticucci, M., and Raga, G.B. 2018. 'Regional climate of the Subtropical Central Andes using high-resolution CMIP5 models. Part II: Future projections for the twenty-first century'. *Climate Dynamics* 51(7), pp. 2913–2925. Available at: https://doi.org/10.1007/s00382-017-4056-4.